The Astrophysical Journal, 616:L163–L166, 2004 December 1

DISCOVERY OF CO GAS IN THE INNER DISK OF TW HYDRAE

Terrence W. Rettig and Joe Haywood
Center for Astrophysics, University of Notre Dame, Notre Dame, IN 46556; trettig@nd.edu
Theodore Simon
Institute for Astronomy, University of Hawaii, 2680 Woodlawn Drive, Honolulu, HI 96822
and
Sean D. Brittain and Erika Gibb
Center for Astrophysics, University of Notre Dame, Notre Dame, IN 46556
Received 2004 August 10; accepted 2004 October 10; published 2004 October 25

ABSTRACT

We report the detection of rovibrationally excited CO emission from the inner disk of the classical T Tauri star (cTTS) TW Hya. We observe ∼6×10^{21} g of CO gas with a rotational temperature of 430 ± 40 K. The linearity of the excitation plot suggests that the CO is optically thin. Atypical for cTTSs, hot CO was not detected, implying that TW Hya has cleared its inner disk region out to a radial distance of ∼0.5 AU. We discuss implications for the structure of the disk as it relates to replenishment and planet formation.

Subject headings: molecular data — planetary systems: protoplanetary disks — stars: individual (TW Hydrae)

1. INTRODUCTION

TW Hya is an isolated classical T Tauri star (cTTS) and the foremost member of the TW Hydrae association (TWA; Rucinski & Krautter 1983). The nearest dark cloud to the TWA is located approximately 13° away (Hoff et al. 1998; Feigelson 1996). At a distance of 56 ± 7 pc (Wichmann et al. 1998), TW Hya has a spectral classification of K7 Ve (Rucinski & Krautter 1983) and an effective temperature of 4150 K (Torres et al. 2003; Trilling et al. 2001; Rucinski & Krautter 1983).

The spectrum of TW Hya exhibits strong, broad Hα emission (FWHM ∼ 200 km s^{-1}) and Li I λ6708 absorption, which is unambiguous and typical of cTTSs with ongoing accretion (Muzerolle et al. 2000; Webb et al. 1999; Reipurth et al. 1996; Rucinski & Krautter 1983), yet the derived age is between 7 and 15 Myr (van Dishoeck et al. 2003; Webb et al. 1999; Hoff et al. 1998). Weakening and narrowing of Hα emission and the concurrent disappearance of the accretion disk supplying the gas marks the transition from the classical to weak-lined T Tauri phase (Muzerolle et al. 2000). The majority of pre–main-sequence stars show few signs of a hot inner disk and ongoing accretion after an age of ∼3–6 Myr (Haisch et al. 2001; Feigelson 1996), but in some cases such activity is observed to survive even at ages as old as 8 Myr (Lyo et al. 2003; see also Strom et al. 1993). Despite its large UV excess (Herczeg et al. 2004), the disk around TW Hya has survived for ∼8–10 Myr, somewhat inconsistent with the disk dispersal theory (Hollenbach et al. 2000).

Estimates of the accretion rate for TW Hya vary from 2×10^{-9} to 5×10^{-10} $M_\odot$ yr^{-1} (Herczeg et al. 2004; Alencar & Batalha 2002; Muzerolle et al. 2000), 10–100 times lower than those estimated for younger stars in Taurus (see Kenyon & Hartmann 1995; Gullbring et al. 1998). Why some stars maintain a long-lived disk activity and others do not is not clear but may be associated with planet formation (Muzerolle et al. 2000).

TW Hya is one of four members of the TWA to have an infrared excess, implying the presence of warm circumstellar dust around the star (Weinberger et al. 2004; Jayawardhana et al. 1999). Images of TW Hya in visible, near-infrared, and millimeter wavelengths reveal a nearly face-on optically thick dust disk (Alencar & Batalha 2002; Weinberger et al. 2002; Trilling et al. 2001; Krist et al. 2000; Wilner et al. 2000; Zuckerman et al. 1995). The presence of a significant amount of gas in the circumstellar disk has been shown by the detection of numerous volatile molecules observed in emission, e.g., H_2 (Weintraub et al. 2000), CO, ^{13}CO, CN, HCN, HCO^+ (Kastner et al. 1997; Zuckerman et al. 1995; Weintraub et al. 1989), and DCO^+ (van Dishoeck et al. 2003). However, these measurements provide very little information concerning the inner disk region. From an analysis of the observed spectral energy distribution (SED) of TW Hya, Calvet et al. (2002) estimated the total outer disk mass to be 0.06 $M_\odot$ (see also Wilner et al. 2000 and Trilling et al. 2001) and concluded that the inner disk within 4 AU of the star is relatively cleared of micron-sized dust. Herczeg et al. (2004) modeled the H_2 emission lines observed in far-ultraviolet spectra of TW Hya and concluded that the strong Lyα emission of the star warms the inner disk surface, located at a radius of $r \sim 2$ AU in the planet-forming region, to a temperature of ∼2500 K.

In this work, we are concerned only with the warm inner disk region, from which we have observed CO emission. Below, we present the results of high-resolution near-infrared observations of the $v = 1$–0 rovibrational band of CO in emission near 4.7 μm. We calculate the rotational temperature and column density of the observed gas. We conclude with a discussion of the implications and potential replenishment scenarios.

2. OBSERVATIONS AND DATA ANALYSIS

Observations of TW Hya were made at the W. M. Keck Observatory on 2003 March 17 using the NIRSPEC spectrometer at a resolving power of ∼25,000 (McLean et al. 1998). For each grating setting, a series of flats and darks was taken to remove systematic effects. The 24 minute integration time produced a signal-to noise ratio of ∼25 for each of the orders presented in Figure 1. The images were cleaned of hot and dead pixels as well as cosmic-ray hits and were then resampled spectrally and spatially so that the spectral and spatial dimensions in the resulting images were orthogonal, falling along rows and columns, respectively (DiSanti et al. 2001; Brittain et al. 2003). Absolute flux calibration was achieved through observation and reduction of standard stars.

In order to cancel most of the atmosphere and background

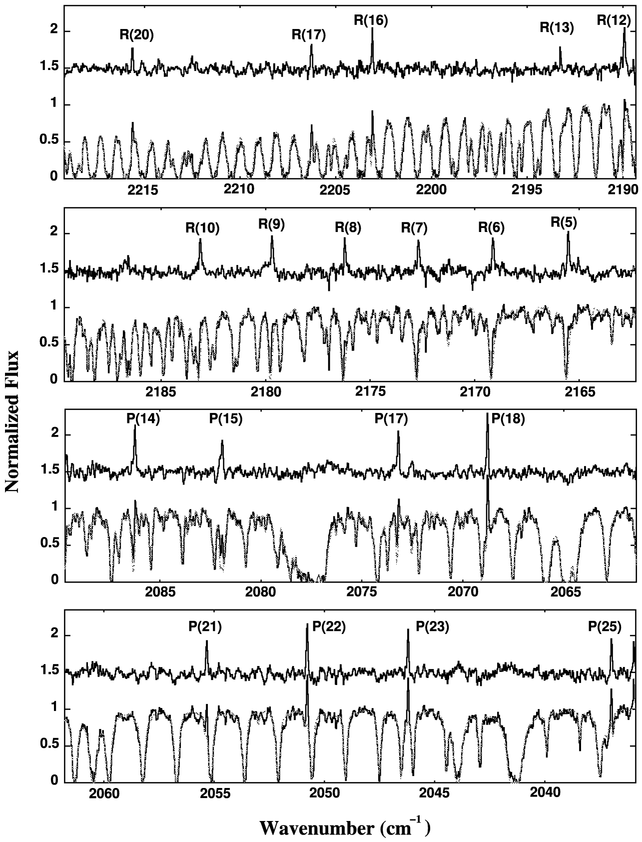

FIG. 1.—Normalized spectrum with the atmospheric transmittance model overplotted. The normalized residual, offset vertically by +1.5, is plotted above. The atmospheric transmittance function of the combined spectrum was modeled using the SSP (Kunde & Maguire 1974), which accesses the updated HITRAN 2000 database (Rothman et al. 2003) and establishes the column burden of the absorbing atmospheric species, the spectral resolving power, and the wavelength calibration. Subtraction of the optimized model (scaled to the observed continuum) reveals the residual of emission lines.

effects, the telescope was nodded by 15″ along the slit from an A to a B position. Each step corresponds to 1 minute of integration. Combining the scans as (A − B − B + A)/2 cancels the telluric features to first order. Subsequently, the FWHM of the spatial profiles in the A and B rows are extracted to obtain the spectra for both positions. For each grating setting, the optimized atmospheric Spectrum Synthesis Program (SSP; Kunde & Maguire 1974), which accesses the updated HITRAN 2000 database (Rothman et al. 2003), establishes the column burden of the absorbing atmospheric species, the spectral resolving power, and the wavelength calibration. Subtraction of the SSP model (scaled to the observed continuum; see Brittain et al. 2003) reveals the residual spectrum of emission lines. The spectral extracts for the CO emission lines, as well as residuals, are shown in Figure 1.

To determine the intensity of the emission lines above the Earth's atmosphere, each emission line (Fig. 1 and Table 1) is divided by the atmospheric transmittance at the Doppler-shifted line center. Before this can be accomplished, the line center must be accurately determined because the transmission of the atmosphere rapidly changes with wavelength. As an example, for the $R(13)$ line, the transmission of the atmosphere can vary from 14% to 31% over the uncertainty in the frequency of the line center. The uncertainty in each observed line position is determined from the standard deviation of its position with respect to the corresponding line formed in the Earth's atmosphere and defines a range of wavenumbers over which the transmittance must be determined. Using the fully resolved SSP model, we find the minimum and maximum transmittance over this wavenumber range for each line. We use this range to determine the uncertainty in transmittance. The resulting uncertainty in flux is combined with the stochastic noise in quadrature to determine the total dF (Table 1).

The Doppler shift of each line was determined by comparing the CO emission lines with telluric CO lines. The resultant heliocentric radial velocity for the CO of 12 ± 1 km s^{-1} is in agreement with previous radio measurements (Kastner et al. 1997; Zuckerman et al. 1995) and implies the CO is associated with the star, which has $v_{\rm helio} \sim 12$ km s^{-1} (Torres et al. 2003; Alencar & Batalha 2002).

The CO lines are unresolved in our spectrum of TW Hya, consistent with a face-on orientation of the disk. However, we can use the spatial extent of the lines and the line profiles to minimally constrain the location to within the seeing disk. Because the emission lines are not extended relative to the point-spread function of the star, the spatial resolution is limited by the atmospheric seeing of ∼0″.8 (FWHM in the M band). At the distance of TW Hya, $d = 56$ pc, this translates to a physical size of ∼45 AU and constrains the location of the gas to a radial distance of $r < 23$ AU from the central star. Thus, it is reasonable to infer that the CO gas is located in the disk.

3. CO IN TW HYA

High-resolution infrared spectroscopy of the rovibrational transitions of ^{12}CO (1, 0) emission provides a sensitive probe of warm circumstellar gas. Under the usual assumption of CO as a rigid rotator, the number of molecules $N_{J'}$ in the rotational state J' is related to T, the gas temperature, and N, the number of molecules in all J' states ($v = 1$) by

$$N_{J'} = \frac{N}{Q_r}(2J' + 1)e^{-B[J'(J'+1)]hc/kT},$$

where k is the Boltzmann constant, h is the Planck constant, c is the speed of light, B is a rotational constant for CO (1.9225 cm^{-1}), J' denotes the upper transition state, and $Q_r = kT/hcB$ is the rotational partition function (Herzberg 1950, p. 121).

Figure 2 presents the excitation plot for the observed CO emission lines in TW Hya. The rotational temperature is defined by the reciprocal of the best-fitting least-squares slope. The total column density N in the $v = 1$ state is obtained from the intercept, ln (N/Q_r). The value of $N_{J'}$ is provided in Table 1 for the 19 CO lines plotted in Figure 2 and spans $J' = 6$–24.

From Figure 2, we obtain a rotational temperature of 430 ± 40 K. The linear fit and the nondetection of the $v =$ 2–1 hot-band emission lines imply that the CO gas is optically thin. Solving for N, using the temperature of 430 K to evaluate the partition function, yields a column density of (2.0 ± 0.2) × 10^{11} cm^{-2} in the $v = 1$ state. From the column density of CO in the $v = 1$ state, we can determine the column density of CO in all vibrational states. If we assume the gas is in local thermodynamic equilibrium, an expected condition for warm gas in the inner disk (Najita et al. 2003), the total column density of CO can be determined from

$$P_v = e^{-vhc\tilde{\nu}_0/kT}/Q_v,$$

where P_v is the fractional population in state v, $\tilde{\nu}_0$ is the vibrational constant for CO (2170.21 cm^{-1}), and Q_v is the vibrational

TABLE 1
Characteristics of Observed CO Lines in TW Hya

Line Identification	$\tilde{\nu}_{obs}$ (cm^{-1})	$\tilde{\nu}_{rest}$ (cm^{-1})	Transmission (%)	$F \pm dF$[a] (10^{-17} W m^{-2})	$N_{J'}$[b] (10^{10} cm^{-2})
*R*20	2215.63	2215.7	41	2.4 ± 0.9	0.24 ± 0.09
*R*17	2206.28	2206.35	37	3.4 ± 1.3	0.4 ± 0.1
*R*16	2203.09	2203.16	40	4.6 ± 1.8	0.5 ± 0.2
*R*13	2193.29	2193.36	21	4.1 ± 2.2	0.44 ± 0.24
*R*12	2189.94	2190.02	32	7.8 ± 3.8	0.8 ± 0.4
*R*10	2183.15	2183.22	19	8.3 ± 4.9	0.94 ± 0.55
*R*9	2179.70	2179.77	15	10.9 ± 6.1	1.2 ± 0.7
*R*8	2176.21	2176.28	12	9.8 ± 4.8	1.1 ± 0.6
*R*7	2172.69	2172.76	14	10.8 ± 6.2	1.2 ± 0.7
*R*6	2169.13	2169.20	14	10.4 ± 5.9	1.2 ± 0.7
*R*5	2165.53	2165.60	12	13.5 ± 7.5	1.6 ± 0.9
*P*14	2086.26	2086.32	32	13.1 ± 7.0	1.7 ± 0.9
*P*15	2081.94	2082.00	34	10.4 ± 3.8	1.3 ± 0.5
*P*17	2073.20	2073.26	39	8.4 ± 3.3	1.1 ± 0.4
*P*18	2068.79	2068.85	75	5.5 ± 2.0	0.70 ± 0.26
*P*21	2055.34	2055.40	66	1.6 ± 0.6	0.21 ± 0.08
*P*22	2050.79	2050.85	82	2.0 ± 0.7	0.3 ± 0.1
*P*23	2046.21	2046.28	83	1.7 ± 0.6	0.233 ± 0.085
*P*25	2036.96	2037.03	79	1.20 ± 0.45	0.17 ± 0.06

[a] Fluxes include a transmittance correction.

[b] The column density, $N_{J'}$ is related to the flux by $N_{J'} = 4\pi F_{J'}/\Omega hcA\tilde{\nu}$, where Ω is the solid angle subtended by the beam, 1.5×10^{-11} sr, *h* is the Plank constant, *c* is the speed of light, *A* is the Einstein *A*-coefficient for the transition, and $\tilde{\nu}$ is the frequency at line center.

partition function, given by $[1 - \exp(-hc\tilde{\nu}_0/kT)]^{-1}$. When we use the resultant $P_{v=1} \sim 7 \times 10^{-4}$, the column density of the CO in all vibrational states is $N(CO) \sim 3 \times 10^{14}$ cm^{-2}, which implies an observed mass in CO of $M(CO) \simeq 10^{21}$ g. Note that because the CO emissivity drops with temperature farther out in the disk, we may be detecting only a small fraction of the gas that is actually present around the star.

4. DISCUSSION

TW Hya has been the subject of many observations and much speculation. In general, one can suppose that the low CO column density we detect is likely a sign of the advanced effects of ongoing dust and gas accretion and dissipation in the inner disk region. Calvet et al. (2002) showed that the inner 4 AU of the disk surrounding TW Hya must be optically thin and contains no more than $0.5M_{lunar}$ of 1 μm particles to correctly model the observed SED at 10 μm. They used a standard gas/dust ratio of 100 to estimate a total gas content of ~40 lunar masses. If the dust is uniformly spread out over the 4 AU disk, the dust density is $\sim 3 \times 10^{-15}$ g cm^{-3} and the maximum column density through the inner disk is very small at 0.18 g cm^{-2}. The lifetime of gas in this region is expected to be a few 100,000 years as it slowly drifts inward following nearly Keplerian orbits.

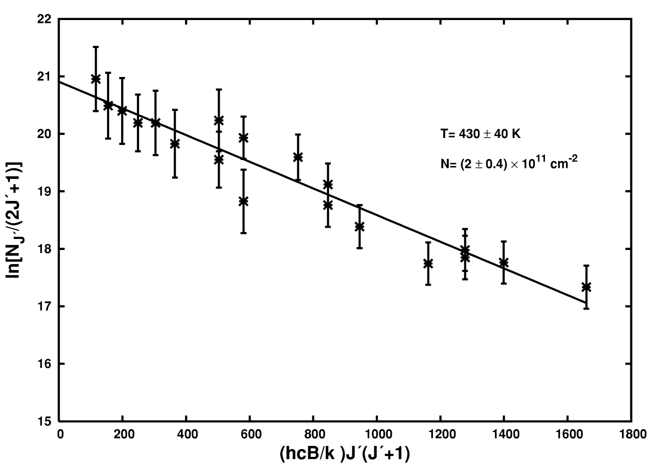

Fig. 2.—Plot of ln $[N_{J'}/(2J'+1)]$ vs. $(Bhc/k)[J'(J'+1)]$ for the CO emission lines observed toward TW Hya. The inverse slope $-(2.3 \pm 0.2) \times 10^{-3}$ of the best-fitting regression line gives the rotational temperature of the gas, and the intercept ln $(N/Q_r) = 20.9 \pm 0.2$ yields the total column density.

The total mass of gas in the inner disk can be determined from the CO column density once the H_2/CO ratio is specified. The H_2/CO ratio in a disk is completely unconstrained, but for illustration we can use the measured diffuse and dense clouds to bracket a plausible range of conditions that are likely to apply to the inner disk region. Using an $H_2/CO \sim 6.7 \times 10^3$ for a dense cloud (Kulesa & Black 2002) gives a total mass estimate of 3×10^{24} g, which corresponds to ~0.1 lunar masses. If we use $H_2/CO \sim 10^7$ (Kulesa & Black 2002 for a diffuse cloud), we get 100 lunar masses (slightly larger than 1 Earth mass). The inferred minimal mass in the inner disk around TW Hya is consistent with the suggestion that it is nearing the end of its accretion stage (Muzerolle et al. 2000).

Obviously, the current inner disk mass is not sufficient to support the observed accretion for millions of years, but the decreased accretion rate is not unreasonable for a star of this age (Muzerolle et al. 2000). Either we are seeing the last gasp of disk clearing as TW Hya transitions to a weak-lined T Tauri star or replenishment is still occurring. For the replenishment case, it may not be unreasonable to assume mass is being transported across a large gap (Artymowicz & Lubow 1996), similar to the scenario that has been described for the circumbinary system DQ Tau (Mathieu et al. 1997) but on a much smaller scale. If indeed, as Calvet et al. (2002) suggest, the inner disk has been cleared by giant planet formation, a massive planet may provide sufficient resonance with the outer disk to facilitate the transport of mass to the accretion disk. The required accretion rate is minimal.

One of the more striking results from this analysis is that the rotational temperature (~400 K) is relatively low compared to other young stars that reveal fundamental CO emission. For example, Najita et al. (2003) present fundamental CO emission from numerous cTTSs with average temperatures ~1200 K. Blake &

Boogert (2004) present similar results for Herbig Ae/Be stars, which all seem to have hot CO and nonlinear excitation plots. Until now, the only known exception to this trend is the transitional Herbig Ae/Be star, HD 141569. For HD 141569, the observed CO rotational temperature is low (∼200 K), the excitation plot is linear, and it has a cleared disk out to about 17 AU (Brittain et al. 2003). An additional clue to the disk structure may be contained in the variability of CO emission. We attempted to observe CO on a previous date 1 yr prior to the present observations and were unable to detect CO above the continuum at a limit of 5%. Current observations show CO as strong as 50% of the continuum, so the CO is likely variable by at least a factor of 10. Neither the periodicity nor the cause of this variability is understood.

From our results, we can only minimally constrain the location of the CO gas. If we assume that the effective temperature of TW Hya (spectral type K7) is ∼4000 K and that the circumstellar gas and dust are in thermodynamic equilibrium, the radial distance within the disk where the blackbody temperature is 400 K is $r \sim 0.5$ AU. Similarly, our preliminary (flat disk) models show that the 400 K CO we are detecting originates from a rather narrow region from 0.5 to 1.0 AU, assuming the gas is in thermal equilibrium with the optically thin dust. The colder gas beyond this distance does not strongly contribute to the observed emission lines unless it is nonthermally excited. Clearly, the observed rotational temperature and potential variability suggest the CO from TW Hya is excited in an environment that is distinct from other cTTSs. The gas distribution and an analysis of the excitation scenarios will be addressed in a future paper.

This work was supported by NSF AST 02-05881. The data presented herein were obtained at the W. M. Keck Observatory, which is operated as a scientific partnership among the California Institute of Technology, the University of California, and the National Aeronautics and Space Administration. The Observatory was made possible by the generous financial support of the W. M. Keck Foundation.

REFERENCES

Alencar, S. H. P., & Batalha, C. 2002, ApJ, 571, 378
Artymowicz, P., & Lubow, S. H. 1996, ApJ, 467, L77
Blake, G. A., & Boogert, A. C. A. 2004, ApJ, 606, L73
Brittain, S. D., et al. 2003, ApJ, 588, 535
Calvet, N., D'Alessio, P., Hartmann, L., Wilner, D., Walsh, A., & Sitko, M. 2002, ApJ, 568, 1008
DiSanti, M. A., Mumma, M. J., Dello Russo, N., & Magee-Sauer, K. 2001, Icarus, 153, 361
Feigelson, E. D. 1996, ApJ, 468, 306
Gullbring, E., Hartmann, L., Briceño, C., & Calvet, N. 1998, ApJ, 492, 323
Haisch, K. E., Lada, E. A., & Lada, C. J. 2001, ApJ, 553, L153
Herczeg, G. J., Wood, B. E., Linsky, J. L., Valenti, J. A., & Johns-Krull, C. M. 2004, ApJ, 607, 369
Herzberg, G. 1950, Molecular Spectra and Molecular Structure, Vol. 1 (2nd ed.; New York: Van Nostrand Reinhold)
Hoff, W., Henning, T., & Pfau, W. 1998, A&A, 336, 242
Hollenbach, D. J., Yorke, H. W., & Johnstone, D. 2000, in Protostars and Planets IV, ed. V. Mannings, A. P. Boss, & S. S. Russell (Tucson: Univ. Arizona Press), 401
Jayawardhana, R., Hartmann, L., Fazio, G., Fisher, R. S., Telesco, C. M., & Piña, R. K. 1999, ApJ, 521, L129
Kastner, J. H., Zuckerman, B., Weintraub, D. A., & Forveille, T. 1997, Science, 277, 67
Kenyon, S. J., & Hartmann, L. 1995, ApJS, 101, 117
Krist, J. E., Stapelfeldt, K. R., Ménard, F., Padgett, D. L., & Burrows, C. J. 2000, ApJ, 538, 793
Kulesa, C. A., & Black, J. H. 2002, in Chemistry as a Diagnostic of Star Formation, ed. C. L. Curry & M. Fich (Ottawa: NRC Press), 60
Kunde, C. A., & Maguire, W. C. 1974, J. Quant. Spectrosc. Radiat. Transfer, 14, 803
Lyo, A. R., Lawson, W. A., Mamajek, E. E., Feigelson, E. D., Sung, E., & Crause, L. A. 2003, MNRAS, 338, 616
Mathieu, R. D., Stassun, K., Basri, G., Jensen, E. L. N., Johns-Krull, C. M., Valenti, J. A., & Hartmann, L. W. 1997, AJ, 113, 1841
McLean, I. S., et al. 1998, Proc. SPIE, 3354, 566
Muzerolle, J., Calvet, N., Briceño, C., Hartmann, L., & Hillenbrand, L. 2000, ApJ, 535, L47
Najita, J., Carr, J. S., & Mathieu, R. D. 2003, ApJ, 589, 931
Reipurth, B., Pedrosa, A., & Lago, M. T. V. T. 1996, A&AS, 120, 229
Rothman, L. S., et al. 2003, J. Quant. Spectrosc. Radiat. Transfer, 82, 5
Rucinski, S. M., & Krautter, J. 1983, A&A, 121, 217
Strom, S. E., Edwards, S., & Skrutskie, M. F. 1993, in Protostars and Planets III, ed. E. H. Levy & J. I. Lunine (Tucson: Univ. Arizona Press), 837
Torres, G., Guenther, E. W., Marschall, L. A., Neuhäuser, R., Latham, D. W., & Stefanik, R. P. 2003, AJ, 125, 825
Trilling, D. E., Koerner, D. W., Barnes, J. W., Ftaclas, C., & Brown, R. H. 2001, ApJ, 552, L151
van Dishoeck, E. F., Thi, W. F., & van Zadelhoff, G. J. 2003, A&A, 400, L1
Webb, R. A., Zuckerman, B., Platais, I., Patience, J., White, R. J., Schwartz, M. J., & McCarthy, C. 1999, ApJ, 512, L63
Weinberger, A. J., Becklin, E. E., Zuckerman, B., & Song, I. 2004, AJ, 127, 2246
Weinberger, A. J., et al. 2002, ApJ, 566, 409
Weintraub, D. A., Kastner, J. H., & Bary, J. S. 2000, ApJ, 541, 767
Weintraub, D. A., Sandell, G., & Duncan, W. D. 1989, ApJ, 340, L69
Wichmann, R., Bastian, U., Krautter, J., Jankovics, I., & Rucinski, S. M. 1998, MNRAS, 301, L39
Wilner, D. A., Ho, P. T. P., Kastner, J. H., & Rodríguez, L. F. 2000, ApJ, 534, L101
Zuckerman, B., Forveille, T., & Kastner, J. H. 1995, Nature, 373, 494